articles

Targeted Delivery of Antisense Inhibitor of miRNA for Antiangiogenesis Therapy Using cRGD-Functionalized Nanoparticles

Xi-Qiu Liu,[†] Wen-Jing Song,[†] Tian-Meng Sun,[‡] Pei-Zhuo Zhang,[§] and Jun Wang*,[†]

Key Laboratory of Brain Function and Diseases of Chinese Academy of Sciences, School of Life Sciences, University of Science and Technology of China, Hefei, Anhui 230027, P. R. China, Hefei National Laboratory for Physical Sciences at the Microscale, University of Science and Technology of China, Hefei, Anhui 230027, P. R. China, and Suzhou GenePharma Co., Ltd, Suzhou, Jiangsu 215123, P. R. China

Abstract: MiRNAs are viable therapeutic targets for cancer therapy, but the targeted delivery of miRNA or its anti-miRNA antisense oligonucleotides (AMOs) remains a challenge. We report here a PEGylated LPH (liposome-polycation-hyaluronic acid) nanoparticle formulation modified with cyclic RGD peptide (cRGD) for specific and efficient delivery of AMO into endothelial cells, targeting $\alpha_v\beta_3$ integrin present on the tumor neovasculature. The nanoparticles effectively delivered anti-miR-296 AMO to the cytoplasm and downregulated the target miRNA in human umbilical vein endothelial cells (HUVECs), which further efficiently suppressed blood tube formulation and endothelial cell migration, owing to significant upregulation of hepatocyte growth factor-regulated tyrosine kinase substrate (HGS), whereas nanoparticles without cRGD modification showed only little AMO uptake and miRNA silencing activity. *In vivo* assessment of angiogenesis using Matrigel plug assay also demonstrated that cRGD modified LPH nanoparticles have potential for antiangiogenesis in miRNA therapeutics. With the delivery of anti-miR-296 AMO by targeted nanoparticles, significant decrease in microvessel formulation within Matrigel was achieved through suppressing the invasion of CD31-positive cells into Matrigel and prompting HGS expression in angiogenic endothelial cells.

Keywords: Anti-miRNA therapy; antiangiogenesis; targeted delivery; cRGD

1. Introduction

The tumor progression goes through two phases, which are separated by the "angiogenic switch".[1] As early as 1971, Judah Folkman had proposed that tumors lay dormant *in situ* for months to years rarely growing beyond 2–3 mm³ in maximum size until the development of neovascularization.[2] When a tumor becomes vascularized, a subgroup of cells switch to an angiogenic phenotype with the emergence of markedly increased tumor growth, tumor cell invasion, and ultimately dissemination.[3–5] Over the past years, thousands of results have been reported on antiangiogenesis for cancer therapy, and some potent compounds have achieved successful clinical trial outcomes.[6–8]

* Corresponding author. Mailing address: School of Life Sciences, University of Science and Technology of China, Hefei, Anhui 230027, P. R. China. E-mail: jwang699@ustc.edu.cn. Tel: (+86) 551-3600335. Fax: (+86) 551-3600402.

† Key Laboratory of Brain Function and Diseases of Chinese Academy of Sciences, School of Life Sciences, University of Science and Technology of China.

‡ Hefei National Laboratory for Physical Sciences at the Microscale, University of Science and Technology of China.

§ Suzhou GenePharma Co., Ltd.

(1) Bergers, G.; Benjamin, L. E. Tumorigenesis and the angiogenic switch. *Nat. Rev. Cancer* **2003**, *3*, 401–410.

(2) Folkman, J. Tumor angiogenesis: therapeutic implications. *New Engl. J. Med.* **1971**, *285*, 1182–1186.

(3) Folkman, J. What is the evidence that tumors are angiogenesis dependent? *J. Natl. Cancer I.* **1990**, *82*, 4–6.

(4) Kerbel, R. S. Tumor angiogenesis: past, present and the near future. *Carcinogenesis* **2000**, *21*, 505–515.

(5) Cooney, M. M.; van Heeckeren, W.; Bhakta, S.; Ortiz, J.; Remick, S. C. Drug Insight: vascular disrupting agents and angiogenesis—novel approaches for drug delivery. *Nat. Clin. Pract. Oncol.* **2006**, *3*, 682–692.

MiRNAs are a class of small noncoding RNAs that regulate huge numbers of transcripts at the posttranscriptional level.[9−11] Abnormal expression of specific miRNAs has been implicated in various human cancers, and miRNA expression profiles have proved useful in tumor classification, prognosis and predicting response to therapy.[12] Up to now, several reports have represented the great potential application of miRNA-based therapy for the treatment in liver and prostate cancers.[12,13] Specific endothelial miRNAs have also been indicated to contribute to angiogenic processes.[14−16] For example, miR-221 and miR-222 inhibit stem cell factor (SCF)-dependent angiogenesis by decreasing the expression of c-KIT, a ligand of the SCF receptor.[16] In contrast, miR-27b and Let-7f are proangiogenic, because inhibition of these miRNAs reduces angiogenic sprouting.[15] Among the angiogenic relevant miRNAs, growth factor-induced miR-296 contributes significantly to angiogenesis by directly targeting the hepatocyte growth factor-regulated tyrosine kinase substrate (HGS) mRNA, leading to decreased levels of HGS and thereby reducing HGS-mediated degradation of the growth factor receptors VEGFR2 and PDGFRβ.[17] To knock down overexpressed miRNA, chemically modified oligonucleotide analogues have been used as miRNA inhibitors including locked nucleic acids (LNA)[18] and 2′-*O*-methyl-,[19] and 2′-*O*-methoxyethyl-modified (2′-MOE) RNA oligonucleotides.[20] However, the poor pharmacokinetic profile, as a consequence of the susceptibility of RNA molecules to serum nucleases, renal clearance and nonspecific biodistribution, restricts systemic applications.[21]

Nanoparticular delivery systems are promising to overcome some hurdles of RNA-based therapeutics delivery, advancing the application of RNA interference in cancer therapy.[21] Among the numerous formulations, a core/shell type of nanoparticle formulation, called liposome−polycation−DNA complex (LPD), was successfully developed in Leaf Huang's lab for delivery of antisense oligodeoxynucleotide (AS-ODN) or siRNA to tumor cells *in vivo*.[22−24] Tumor specificity was further introduced by using a PEGylated lipid tethered to a targeting ligand.[25] Then hyaluronic acid (HA) was chose to improve the nanoparticle formation for reducing the immunotoxicity of the formulation.[26] The PEGylated targeted LPH-NP showed a strong potential to deliver oligonucleotides for cancer therapy,[26] such as in melanoma[26] and fibrosarcoma treatments.[27]

In principle, active targeting of the tumor vasculature could starve a tumor by choking off its blood supply.[28] In this study, to demonstrate the therapeutic potential of interrupting miR-296 induced angiogenesis by targeted delivery of anti-miR-296 AMO to endothelial cells, we developed LPH-NP

(6) Zhe Wang, P. C. H. A nanocapsular combinatorial sequential drug delivery system for antiangiogenesis and anticancer activities. *Biomaterials* **2010**, *31*, 7115–7123.

(7) Kerbel, R. S.; Kamen, B. A. The anti-angiogenic basis of metronomic chemotherapy. *Nat. Rev. Cancer* **2004**, *4*, 423–436.

(8) Hurwitz, H.; Fehrenbacher, L.; Novotny, W.; Cartwright, T.; Hainsworth, J.; Heim, W.; Berlin, J.; Baron, A.; Griffing, S.; Holmgren, E.; Ferrara, N.; Fyfe, G.; Rogers, B.; Ross, R.; Kabbinavar, F. Bevacizumab plus irinotecan, fluorouracil, and leucovorin for metastatic colorectal cancer. *N. Engl. J. Med.* **2004**, *350*, 2335–2342.

(9) Mourelatos, Z. Small RNAs - The seeds of silence. *Nature* **2008**, *455*, 44–45.

(10) Filipowicz, W.; Bhattacharyya, S. N.; Sonenberg, N. Mechanisms of post-transcriptional regulation by microRNAs: are the answers in sight? *Nat. Rev. Genet.* **2008**, *9*, 102–114.

(11) Zhao, Y.; Srivastava, D. A developmental view of microRNA function. *Trends Biochem. Sci.* **2007**, *32*, 189–197.

(12) Kota, J.; Chivukula, R. R.; O'Donnell, K. A.; Wentzel, E. A.; Montgomery, C. L.; Hwang, H. W.; Chang, T. C.; Vivekanandan, P.; Torbenson, M.; Clark, K. R.; Mendell, J. R.; Mendell, J. T. Therapeutic microRNA delivery suppresses tumorigenesis in a murine liver cancer model. *Cell* **2009**, *137*, 1005–1017.

(13) Takeshita, F.; Patrawala, L.; Osaki, M.; Takahashi, R.; Yamamoto, Y.; Kosaka, N.; Kawamata, M.; Kelnar, K.; Bader, A. G.; Brown, D.; Ochiya, T. Systemic delivery of synthetic microRNA-16 inhibits the growth of metastatic prostate tumors via downregulation of multiple cell-cycle genes. *Mol. Ther.* **2010**, *18*, 181–187.

(14) Suarez, Y.; Fernandez-Hernando, C.; Pober, J. S.; Sessa, W. C. Dicer dependent microRNAs regulate gene expression and functions in human endothelial cells. *Circ. Res.* **2007**, *100*, 1164–1173.

(15) Kuehbacher, A.; Urbich, C.; Zeiher, A. M.; Dimmeler, S. Role of dicer and drosha for endothelial MicroRNA expression and angiogenesis. *Circ. Res.* **2007**, *101*, 59–68.

(16) Poliseno, L.; Tuccoli, A.; Mariani, L.; Evangelista, M.; Citti, L.; Woods, K.; Mercatanti, A.; Hammond, S.; Rainaldi, G. MicroRNAs modulate the angiogenic properties of HLTVECs. *Blood* **2006**, *108*, 3068–3071.

(17) Wurdinger, T.; Tannous, B. A.; Saydam, O.; Skog, J.; Grau, S.; Soutschek, J.; Weissleder, R.; Breakefield, X. O.; Krichevsky, A. M. MiR-296 regulates growth factor receptor overexpression in angiogenic endothelial cells. *Cancer Cell* **2008**, *14*, 382–393.

(18) Vester, B.; Wengel, J. LNA (Locked nucleic acid): High-affinity targeting of complementary RNA and DNA. *Biochemistry* **2004**, *43*, 13233–13241.

(19) Krutzfeldt, J.; Rajewsky, N.; Braich, R.; Rajeev, K. G.; Tuschl, T.; Manoharan, M.; Stoffel, M. Silencing of microRNAs *in vivo* with 'antagomirs'. *Nature* **2005**, *438*, 685–689.

(20) Esau, C.; Davis, S.; Murray, S. F.; Yu, X. X.; Pandey, S. K.; Pear, M.; Watts, L.; Booten, S. L.; Graham, M.; McKay, R.; Subramaniam, A.; Propp, S.; Lollo, B. A.; Freier, S.; Bennett, C. F.; Bhanot, S.; Monia, B. P. MiR-122 regulation of lipid metabolism revealed by *in vivo* antisense targeting. *Cell Metab.* **2006**, *3*, 87–98.

(21) Howard, K. A. Delivery of RNA interference therapeutics using polycation-based nanoparticles. *Adv. Drug Delivery Rev.* **2009**, *61*, 710–720.

(22) Chen, Y. C.; Sen, J.; Bathula, S. R.; Yang, Q.; Fittipaldi, R.; Huang, L. Novel cationic lipid that delivers siRNA and enhances therapeutic effect in lung cancer cells. *Mol. Pharm.* **2009**, *6*, 696–705.

(23) Li, S. D.; Chono, S.; Huang, L. Efficient oncogene silencing and metastasis inhibition via systemic delivery of siRNA. *Mol. Ther.* **2008**, *16*, 942–946.

(24) Li, S. D.; Chen, Y. C.; Hackett, M. J.; Huang, L. Tumor-targeted delivery of siRNA by self-assembled nanoparticles. *Mol. Ther.* **2008**, *16*, 163–169.

(25) Li, S. D.; Huang, L. Targeted delivery of antisense oligodeoxynucleotide and small interference RNA into lung cancer cells. *Mol. Pharmaceutics* **2006**, *3*, 579–588.

formulation modified with cyclic RGD peptide (cRGD). cRGD can efficiently target $\alpha_v\beta_3$ integrin present on the surface of angiogenic endothelial cells and is known to enhance the delivery of doxorubicin to tumor neovasculature.[29−32] However, there are no reports on targeted delivery of anti-miRNA AMO for antiangiogenesis therapy. In the present study, we have developed cRGD-LPH-NP to specifically deliver anti-miR-296 AMO to $\alpha_v\beta_3$ integrin-positive angiogenic endothelial cells. We have shown that significantly increasing cellular uptake of anti-miRNA AMO leads to profound downregulation of miR-296 and antiangiogenesis effects both *in vitro* and *in vivo*. These results indicate that the suppression of miR-296 in endothelial cells by targeted anti-miRNA AMO delivery could provide an efficient strategy for antiangiogenesis therapy in cancer treatment.

2. Materials and Methods

2.1. Materials. Distearoylphosphatidylcholine (DSPC), cholesterol, 1,2-distearoyl-*sn*-glycero-3-phosphoethanolamine-*N*-[methoxy(polyethyleneglycol)-2000] (DSPE-PEG2000) and 1,2-distearoyl-*sn*-glycero-3-phosphoethanolamine-*N*-[maleimide(polyethylene glycol)-2000] (DSPE-PEG2000-maleimide) were purchased from Avanti Polar Lipids, Inc. (Alabaster, AL). Protamine sulfate (fraction X from salmon) and hyaluronic acid sodium salt from *Streptococcus equi* (HA) were purchased from Sigma-Aldrich (St. Louis, MO). The cyclic 5mer RGD *c*[RGDfK (Ac-SCH$_2$CO)] was synthesized by Peptides International (Louisville, KY, USA). The peptide was equipped with thioacetyl group. As described by Schiffelers et al., acetyl-protected peptide was deacetylated in an aqueous solution of 0.05 M Hepes/0.05

M hydroxylamine-HCl/0.03 mM ethylenediamine tetraacetic acid (EDTA) of pH 7.0 for 30 min at room temperature.[32] Next, DSPE-PEG2000-cRGD was synthesized by incubating the activated peptide with the DSPE-PEG2000-maleimide overnight at 4 °C. Cholesteryl (2-[bis(2-hydroxyethyl)-ammonium] ethyl) carbamate iodide (BHEM-Chol) was synthesized according to the literature.[33]

Anti-miR-296 AMO and mismatch AMO were synthesized by GenePharma Co. Ltd. (Shanghai, China). Anti-miR-296 AMO targets the miR-296 sequence 14-AGGGCCCCCCCU-CAAUCCUGU-34 (http://microrna.sanger.ac.uk). The mismatch sequence does not match any human genome sequence. FAM-labeled RNA oligonucleotide and Cy3-labeled RNA oligonucleotide were also obtained from GenePharma Co. Ltd.

2.2. Cells and Animals. Human umbilical vein endothelial cells (HUVECs) expressing $\alpha_v\beta_3$ integrin[34] were obtained from Invitrogen. The cells were maintained in Medium 200 (Invitrogen) supplemented with low serum growth supplement (LSGS, Invitrogen).

Female BALB/c nude mice (6−8 weeks, weighing 20−24 g) were obtained from Experimental Animal Center, Chinese Science Academy (Shanghai, China). All animals received care in compliance with the guidelines outlined in the *Guide for the Care and Use of Laboratory Animals*, and the procedures were approved by the University of Science and Technology of China Animal Care and Use Committee.

2.3. Preparation of Nontargeted LPH-NP or cRGD-LPH-NP. The schematic illustration of nanoparticle preparations is shown in Scheme 1. Liposome-protamine-HA nanoparticles (LPH-NP) were first prepared as follows based on a previous description by Chono et al.[26] Small unilamellar liposomes consisting of BHEM-Chol, cholesterol, DSPC and DSPE-PEG2000 (molar ratio = 40:48:10:2) were first prepared by thin film hydration followed by sonication for 20 min. The total lipid concentration was fixed at 5 mg/mL. To prepare complex of AMO/HA and protamine, 36 μL of protamine (200 μg/mL) and 43 μL of a mixture of AMO and HA (170 μg/mL, weight ratio = 1:1) were mixed in a 1.5 mL tube. The complex was allowed to stand at room temperature for 10 min before the addition of 42 μL of liposome solution (5 mg/mL) prepared as above. The formulation was termed as the naked LPH-NP. The naked LPH-NP formulation was kept at room temperature for another 10 min for further application.

Nontargeted LPH-NP and cRGD-LPH-NP were prepared by incubating the naked LPH-NP suspension with 10.6 μL of micellar solution of DSPE-PEG2000 (10 mg/mL) or mixed solution of DSPE-PEG-cRGD/DSPE-PEG2000 at various ratios at 50 °C for 10 min, respectively, and then allowed to

(26) Chono, S.; Li, S. D.; Conwell, C. C.; Huang, L. An efficient and low immunostimulatory nanoparticle formulation for systemic siRNA delivery to the tumor. *J. Controlled Release* **2008**, *131*, 64–69.

(27) Chen, Y. C.; Wu, J. Z. J.; Huang, L. Nanoparticles Targeted With NGR Motif Deliver c-myc siRNA and Doxorubicin for Anticancer Therapy. *Mol. Ther.* **2010**, *18*, 828–834.

(28) Jain, R. K. Normalizing tumor vasculature with anti-angiogenic therapy: A new paradigm for combination therapy. *Nat. Med.* **2001**, *7*, 987–989.

(29) Singh, S. R.; Grossniklaus, H. E.; Kang, S. J.; Edelhauser, H. F.; Ambati, B. K.; Kompella, U. B. Intravenous transferrin, RGD peptide and dual-targeted nanoparticles enhance anti-VEGF intraceptor gene delivery to laser-induced CNV. *Gene Ther.* **2009**, *16*, 645–659.

(30) Murphy, E. A.; Majeti, B. K.; Barnes, L. A.; Makale, M.; Weis, S. M.; Lutu-Fuga, K.; Wrasidlo, W.; Cheresh, D. A. Nanoparticle-mediated drug delivery to tumor vasculature suppresses metastasis. *Proc. Natl. Acad. Sci. U.S.A.* **2008**, *105*, 9343–9348.

(31) Nasongkla, N.; Shuai, X.; Ai, H.; Weinberg, B. D.; Pink, J.; Boothman, D. A.; Gao, J. M. cRGD-functionalized polymer micelles for targeted doxorubicin delivery. *Angew. Chem., Int. Ed.* **2004**, *43*, 6323–6327.

(32) Schiffelers, R. M.; Koning, G. A.; ten Hagen, T. L. M.; Fens, M. H. A. M.; Schraa, A. J.; Janssen, A. N. P. C. A.; Kok, R. J.; Molema, G.; Storm, G. Anti-tumor efficacy of tumor vasculature-targeted liposomal doxorubicin. *J. Controlled Release* **2003**, *91*, 115–122.

(33) Fang, N.; Wang, J.; Mao, H. Q.; Leong, K. W.; Chan, V. BHEM-Chol/DOPE liposome induced perturbation of phospholipid bilayer. *Colloids Surf., B* **2003**, *29*, 233–245.

(34) Trikha, M.; Zhou, Z.; Timar, J.; Raso, E.; Kennel, M.; Emmell, E.; Nakada, M. T. Multiple roles for platelet GPIIb/IIIa and alpha v beta 3 integrins in tumor growth, angiogenesis, and metastasis. *Cancer Res.* **2002**, *62*, 2824–2833.

Scheme 1. The Procedure Involved in the Preparation of Nontargeted LPH-NP and cRGD-LPH-NP for AMO Delivery
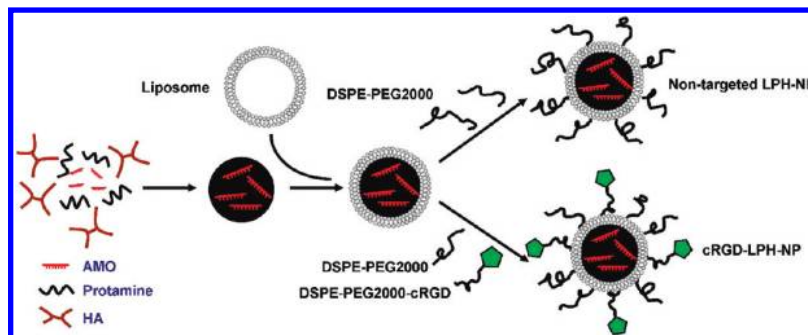
stand at room temperature for 10 min. The resulting LPH-NP and cRGD-LPH-NP formulations were used within 20 min for the following experiments. The particle size and zeta potential of the resulting particles were analyzed as described in section 2.4, and delivery efficiency of the cRGD-LPH-NP of different DSPE-PEG2000-cRGD/DSPE-PEG2000 ratios was determined as described in section 2.5. The optimal ratio of the cRGD-LPH-NP formulation was determined by the results from particle size, zeta potential and *in vitro* delivery efficiency.

2.4. Particle Size and Zeta-Potential Measurements. Measurements of particle size and zeta potential of nanoparticles were performed using a Zetasizer Nano ZS90 (Malvern Instruments, U.K.). Different formulations were freshly prepared before measurements according to the procedure described above. The size measurement was performed at 25 °C at a 90° scattering angle. The mean hydrodynamic diameter was determined by cumulative analysis. The zeta-potential measurements were performed using an aqueous dip cell in an automatic mode.

2.5. In Vitro Intracellular AMO Delivery Study. HUVECs (5×10^4) were seeded in a 24-well tissue culture plate (Corning Inc., Corning, NY) 24 h before experiments. HUVECs were seeded at 5×10^4 cells/well in a 24-well tissue culture plate for 24 h. Different formulations, including free FAM-labeled RNA oligonucleotide, FAM-labeled RNA oligonucleotide in nontargeted LPH-NP and cRGD-LPH-NP, were added to each well giving a final RNA oligonucleotide concentration of 240 nM. After 5 h incubation, cells were washed three times with PBS, and then collected by detaching them from wells using 0.025% trypsin and 0.01% EDTA. Cells were finally resuspended in 200 μL of PBS for flow cytometric analysis using a Becton Dickinson FACSCalibur flow cytometer. For each experiment, 10,000 FAM-positive events were collected and analyzed using WinMDI 2.9 software.

For microscopic observation, HUVECs (5×10^4) were seeded on coverslips in a 24-well tissue culture plate and transfected 24 h later with nontargeted LPH-NP or cRGD-LPH-NP loaded with 240 nM of Cy3-labeled RNA oligonucleotide, or 240 nM free Cy3-labeled RNA oligonucleotide for 5 h in 0.5 mL of Medium 200 containing LSGS. Cells were washed and fixed with 4% paraformaldehyde, and F-actin was labeled by Alexa Fluor 488 phalloidin (Invitrogen). The nuclei were counterstained with 4′,6-diamidino-2-phenylindole (DAPI). The

slides were mounted and observed with a Zeiss LSM510 laser confocal scanning microscope imaging system (Germany) with an upright confocal microscope and a 40× objective.

2.6. In Vitro MiR-296 Inhibition Study. HUVECs (3×10^5) were seeded in a 6-well tissue culture plate (Corning Inc., Corning, NY) 24 h before experiments. Cells were incubated with free anti-miR-296 AMOs, anti-miR-296 AMO in nontargeted LPH-NP, anti-miR-296 AMO in cRGD-LPH-NP and mismatch AMO in cRGD-LPH-NP at 37 °C for 24 h. The concentration of anti-miRNA AMO was 500 nM.

Total RNA was isolated and an RNA fraction highly enriched in RNA species ≤200 nt was obtained according to the mirVana miRNA isolation kit (Applied Biosystems). Equal amounts of small RNAs were converted into cDNA using miR-296 and U6 snRNA RT primers (Applied Biosystems, using the manufacturer's protocol). Subsequently, PCR was performed using primers and materials from Applied Biosystems to determine the expression level change of miR-296 in HUVECs.

2.7. Western Blotting Analysis of MiR-296 Targeted Protein. HUVECs were transfected with 500 nM anti-miR-296 AMO or mismatch AMO in different formulations for 48 h in a similar way as described above. Cells were lysed and proteins (50 μg) of whole cell lysate were treated with an electrophoresis loading buffer containing 5% (w/v) 2-mercaptoethanol, following analysis by SDS−PAGE. After electrophoresis, proteins were electrophoretically transferred to Immobilon transfer membrane (Millipore) and preincubated with a blocking reagent (5% skim milk) at room temperature for 1 h. Subsequently, the membrane was divided into two parts and incubated separately with primary antibodies for β-actin and HGS (1:5000 and 1:1000 dilution, respectively, Santa Cruz Biotechnology and Abcam) overnight at 4 °C. They were labeled with horseradish peroxidase conjugated-antibody to mouse IgG and to rabbit IgG (1:5000 dilution, Santa Cruz Biotechnology) at room temperature for 1 h. The chemiluminescence detection was then performed using SuperSignal West Pico Chemiluminescent Substrate (Pierce).

2.8. In Vitro Angiogenesis Assay. HUVECs (passaged fewer than seven times) were transfected with anti-miR-296 AMO or mismatch AMO using different formulations. At 5 h after transfection, HUVECs were seeded on Matrigel (Becton Dickinson). After 12 or 24 h incubation, pictures

of tubule formation were taken using a digital camera system coupled to a microscope with a 20× objection. The experiments were performed in triplicate, repeated at least twice.

2.9. *In Vitro* Migration Assay. Confluent HUVECs (passaged fewer than seven times) were transfected with anti-miR-296 AMO or mismatch AMO using different formulations. At 5 h after transfection, a cell scratch spatula was used to make a scratch in the cell monolayer, and then the cell monolayers were rinsed gently by PBS and further incubated. Pictures of the scratches were taken using a digital camera system coupled to a microscope with a 20× objection. The cells were incubated for 6 and 16 h, after which pictures were taken again.

2.10. *In Vivo* Assessment of Angiogenesis Using Matrigel Plug Assay. The Matrigel plug assay was performed to assess *in vivo* angiogenesis.[35−37] Briefly, growth factor-reduced Matrigel (BD Biosciences) was mixed with 1 μg/mL basic fibroblast growth factor (Invitrogen) and 1000 pmol of anti-miR-296 AMO or mismatch AMO in different formulations. The Matrigel mixture was injected subcutaneously on the back of female BALB/c nude mice. All of the treatment groups consisted of three mice. After 7 days, mice were sacrificed, while the Matrigel plugs were removed, and photographed.

The plugs were further fixed in 4% paraformaldehyde, embedded in paraffin and sectioned for immunohistochemistry of HGS. Sections were deparaffinized and pretreated by boiling in 10 mM citrate buffer (pH 6.0) for 20 min at 750 W in a microwave oven. Tissue peroxidase activity was quenched by incubation in 3% H_2O_2 in PBS for 10 min, followed by blocking in 10% serum of the secondary antibody species. Immunohistochemistry was performed with a goat anti-mouse HGS antibody (1:100 dilution, Abcam). Positive reactions were developed using DAB as a peroxidase substrate. Sections were counterstained in Mayer's hematoxylin, dehydrated, and coverslipped in resin. The HGS staining was observed by an optical microscope (Nikon TE2000-U, Japan) in randomly selected fields (20× objective).

Microvessels within Matrigel were also assessed by CD31 immunostaining on frozen sections with 8 μm. After rinsing and blocking, the sections were incubated with a goat anti-mouse CD31 monoclonal antibody (Santa Cruz Biotechnol-

ogy) at 1:100 dilution, followed by incubation with rhodamine-conjugated secondary rabbit anti-goat IgG (Santa Cruz, CA, USA) at 1:200 dilution. The slides were counterstained with DAPI. CD31 positive endothelial cells were observed with a Zeiss LSM510 laser confocal scanning microscope imaging system (Germany) with an upright confocal microscope and a 40× objective.

3. Results and Discussion

3.1. Optimization of cRGD-LPH-NP Formulations. Here we used a novel liposome, which contained BHEM-Chol, cholesterol, DSPC and DSPE-PEG2000, to prepare nontargeted LPH-NP and cRGD-LPH-NP. BHEM-Chol has been proved great potential of effectively fusing with cell membrane as a membrane perturbant.[33] The liposome has been demonstrated to achieve comparable transfection efficiency but lower cytotoxicity in various cell lines in comparison with other commercial liposomal system such as Lipofectamine 2000 (data not shown).

We prepared formulations of AMO in cRGD-LPH-NP at different molar ratios of DSPE-PEG2000-cRGD/DSPE-PEG2000 and analyzed their particle size and zeta potential. The results are shown in Figures 1A and 1B. Increase of the ratio of DSPE-PEG2000-cRGD to DSPE-PEG2000 slightly decreased zeta potential. Large particles with the diameter above 100 nm were found at the molar ratio of 1:7.5, and increase of DSPE-PEG2000-cRGD in the formulation of cRGD-LPH-NP decreased the particle size from 109 to 80 nm with a sharp change at the molar ratio between 1:7.5 and 1:5.0, and then the particle size remained stable around 80 nm as the continuous increase of DSPE-PEG2000-cRGD. To further investigate which ratio resulted in the optimal cRGD-LPH-NP formulation, we encapsulated FAM-labeled RNA oligonucleotide in the cRGD-LPH-NP formulation prepared at different DSPE-PEG2000-cRGD/DSPE-PEG2000 molar ratios and determined their delivery efficiency *in vitro*. Flow cytometric assay was used to study the uptake of nanoparticles into HUVECs which overexpress the $a_v\beta_3$ integrin.[34] The cellular internalization efficiency was quantified by the enhancement of relative geometrical mean fluorescence intensity (GMFI) of cRGD-LPH-NP to that of nontargeted LPH-NP (Figure 1C). At the molar ratio of 1:5.0, a 5.5-fold enhancement in GMFI was achieved with the treatment of cRGD-LPH-NP relative to the treatment of nontargeted LPH-NP, which was a significant increase in relative GMFI when compared with the molar ratio of 1:7.5 ($p < 0.05$). However, further increasing DSPE-PEG2000-cRGD no longer significantly increased the relative GMFI, suggesting that more targeted cRGD moiety of cRGD-LPH-NP would not lead to higher delivery efficiency. Therefore, we chose 1:5.0 as the optimal molar ratio of DSPE-PEG2000-cRGD to DSPE-PEG2000 for the preparation of cRGD-LPH-NP in the following experiments.

3.2. Uptake of cRGD-LPH-NP by Endothelial Cells through Receptor-Mediated Internalization. Figure 2A shows the fluorescence images of HUVECs after 5 h

(35) Wong, R. J.; Chan, M. K.; Yu, Z. K.; Ghossein, R. A.; Ngai, I.; Adusumilli, P. S.; Stiles, B. M.; Shah, J. P.; Singh, B.; Fong, Y. Angiogenesis inhibition by an oncolytic herpes virus expressing interleukin 12. *Clin. Cancer Res.* **2004**, *10*, 4509–4516.

(36) Donate, F.; Juarez, J. C.; Guan, X. J.; Shipulina, N. V.; Plunkett, M. L.; Tel-Tsur, Z.; Shaw, D. E.; Morgan, W. T.; Mazar, A. P. Peptides derived from the histidine-proline domain of the histidine-proline-rich glycoprotein bind to tropomyosin and have antiangiogenic and antitumor activities. *Cancer Res.* **2004**, *64*, 5812–5817.

(37) Varet, J.; Vincent, L.; Akwa, Y.; Mirshahi, P.; Lahary, A.; Legrand, E.; Opolon, P.; Mishal, Z.; Baulieu, E. E.; Soria, J.; Soria, C.; Li, H. Dose-dependent effect of dehydroepiandrosterone, but not of its sulphate ester, on angiogenesis. *Eur. J. Pharmacol.* **2004**, *502*, 21–30.
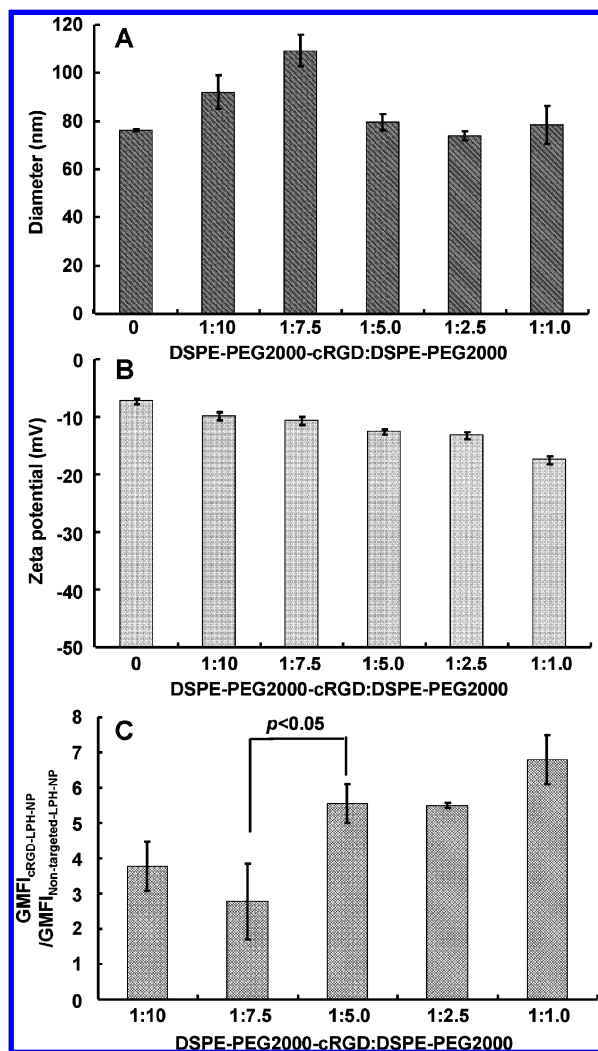
Figure 1. Optimization of cRGD-LPH-NP for AMO delivery: (A and B) effect of molar ratio of DSPE-PEG2000-cRGD to DSPE-PEG2000 on particle size (A) and zeta potential (B) of cRGD-LPH-NP; (C) effect of molar ratio of DSPE-PEG2000-cRGD to DSPE-PEG2000 on uptake of AMO by HUVECs. The student's *t* test was performed ($n = 3$).

Figure 2. Cellular uptake of AMO *in vitro* with the delivery of cRGD-LPH-NP or nontargeted LPH-NP: (A) Fluorescence photographs of HUVECs after 5 h incubation with Cy3-labeled RNA oligonucleotide in cRGD-LPH-NP or in nontargeted LPH-NP (blue, DAPI stained nucleus; green, Alexa Fluor 488 phalloidin stained F-actin; red, Cy3-labeled RNA oligonucleotide); (B) flow cytometric analyses of cellular fluorescence intensity of HUVECs incubated with different formulations containing FAM-labeled RNA oligonucleotide at 37 °C for 5 h.

incubation at 37 °C with Cy3-labeled RNA oligonucleotide in cRGD-LPH-NP and nontargeted LPH-NP. The intensity of red fluorescence observed in HUVECs incubated with cRGD-LPH-NP was markedly higher when compared with that of HUVECs incubated with nontargeted LPH-NP. This phenomenon demonstrated that the ligand−receptor recognition between cRGD and $\alpha_v\beta_3$ integrin mediated the surface binding of nanoparticles to HUVECs,[32,38] and probably induced cRGD-LPH-NP to enter cells through caveolae and localize in the perinuclear regions.[39] It is possible that negatively charged surface of nontargeted LPH-NP resulted in electrostatic repulsion to cells, which in fact is unfavorable for binding to cell surface.[40] Therefore, without receptor mediation, nontargeted LPH-NP had less opportunity to reach HUVEC cell surface and be internalized into cells. However, the delivered Cy3-labeled RNA oligonucleotide appeared as punctate spots in this observation, indicating that the particles
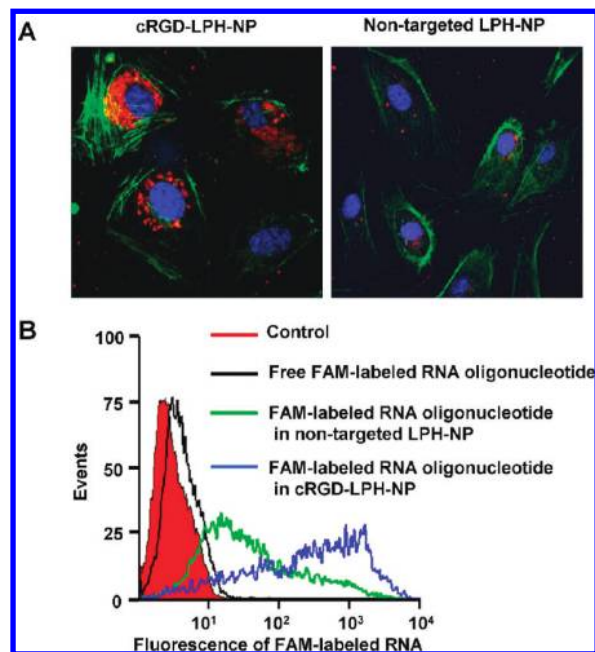
and RNA oligonucleotide may be still trapped within endosome after 5 h incubation. The escape activity of nanoparticles or RNA oligonucleotide from endosome is not clear at the present time and needs further investigation.

In another study, the internalizations of free FAM-labeled RNA oligonucleotide, FAM-labeled RNA oligonucleotide in nontargeted LPH-NP and cRGD-LPH-NP were also monitored by flow cytometric analyses (Figure 2B). Incubation of nontargeted LPH-NP with HUVECs resulted in slight increase of cellular fluorescence, and the percentage of cell population with log mean fluorescence intensity more than 10^2 was only 24.46%. In contrast, cell population with high fluorescence was more than 70% when HUVECs were incubated with cRGD-LPH-NP. It further confirmed the

(38) Dechantsreiter, M. A.; Planker, E.; Matha, B.; Lohof, E.; Holzemann, G.; Jonczyk, A.; Goodman, S. L.; Kessler, H. N-methylated cyclic RGD peptides as highly active and selective alpha(v)beta(3) integrin antagonists. *J. Med. Chem.* **1999**, *42*, 3033–3040.

(39) Sahay, G.; Alakhova, D. Y.; Kabanov, A. V. Endocytosis of nanomedicines. *J. Controlled Release* **2010**, *145*, 182–195.

(40) Wang, Y. C.; Liu, X. Q.; Sun, T. M.; Xiong, M. H.; Wang, J. Functionalized micelles from block copolymer of polyphospho-ester and poly(epsilon-caprolactone) for receptor-mediated drug delivery. *J. Controlled Release* **2008**, *128*, 32–40.
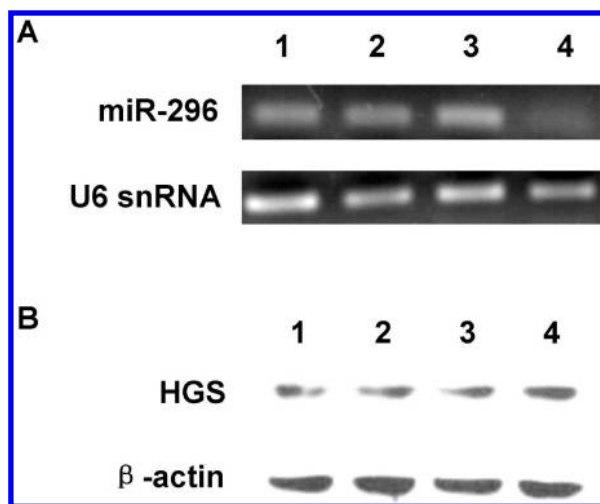
Figure 3. Intracellular miR-296 expression and HGS expression regulated by different formulations *in vitro*: (A) RT-PCR analysis of miR-296 in HUVECs after treatments with different formulations containing anti-miR-296 AMO or mismatch AMO for 24 h; (B) Western blot analysis of HGS expression in HUVECs after treatments with different formulations containing anti-miR-296 AMO or mismatch AMO for 48 h (1, untreated control; 2, anti-miR-296 AMO in nontargeted LPH-NP; 3, mismatch AMO in cRGD-LPH-NP; 4, anti-miR-296 AMO in cRGD-LPH-NP).

preponderance of cRGD-LPH-NP on cellular uptake due to the interaction of cRGD and $\alpha_v\beta_3$ integrin.

3.3. Efficient MiR-296 Silencing *in Vitro* and Enhanced HGS Expression by Anti-miR-296 AMO in cRGD-LPH-NP. MiR-296 becomes more abundant in endothelial cells in response to angiogenic factors produced by cancer cells. We performed RT-PCR analysis of miR-296 in HUVECs after 24 h transfection with different formulations containing anti-miR-296 AMO or mismatch AMO. The expression pattern of miR-296 was almost concordant with the control group when HUVECs were transfected with anti-miR-296 AMO in nontargeted LPH-NP or mismatch AMO in cRGD-LPH-NP (Figure 3A). However, no visible band of miR-296 was detectable when the cells were transfected with anti-miR-296 AMO in cRGD-LPH-NP. This result indicated that the silencing activity was ligand dependent and only specific delivery of anti-miR-296 AMO with targeted cRGD-LPH-NP could effectively suppress miR-296 expression.

HGS was one of the highest scored proteins among the predicted miR-296 targets. It has been reported that miR-296 downregulates the synthesis of HGS by directly binding to sites within the 3′UTR of its mRNA.[17] HGS is an endosomal protein essential for the efficient sorting of activated growth factor receptors into the lysosomal degradation pathway. Elevated levels of growth factor receptors on the surface of endothelial cells, usually observed during tumor-induced angiogenesis, suggest a diminished role for

HGS.[41,42] To further demonstrate the biological activity of different formulations by analyzing miR-296-mediated modulation of endogenous HGS, HUVECs were transfected with different formulations containing anti-miR-296 AMO or mismatch AMO. After 48 h, the cell lysates were analyzed for HGS expression levels by Western blotting. Inhibition of miR-296 would result in increased levels of HGS. The HGS protein expression in HUVECs treated with anti-miR-296 AMO in cRGD-LPH-NP was significantly increased, while delivery of anti-miR-296 AMO with nontargeted LPH-NP or delivery of mismatch AMO with cRGD-LPH-NP had almost no effect on the expression of HGS (Figure 3B). The results showed that in HUVECs HGS was expressed at a lower level under angiogenic conditions due to the upregulation of miR-296, and its reduction could be prevented by blocking miR-296 using specific AMO. cRGD-LPH-NP was able to effectively deliver anti-miR-296 AMO into $\alpha_v\beta_3$ integrin-positive endothelial cells, resulting in miR-296 silencing and enhanced HGS expression, while increase of HGS in endothelia cells would be supposed to cause antiangiogenesis effect.

3.4. *In Vitro* Effective Antiangiogenesis with Targeted Delivery of Anti-miR-296 AMO. To address the change of miR-296 function in angiogenesis after specific anti-miR-296 AMO delivery, we examined the angiogenesis of HUVECs in cell culture after transfection with different formulations containing anti-miR-296 AMO or mismatch AMO. HUVECs can differentiate and form capillary-like structures on Matrigel in the presence of bovine calf serum and a mixture of both acidic and basic fibroblast growth factors.[43] The capacity of formation into tubelike vessels can be used to assess compounds that either inhibit or stimulate angiogenesis.[44] Transfected HUVECs were seeded on Matrigel for 12 or 24 h incubation in Medium 200 containing LSGS, and then tubules were visualized under a light microscopy. Tubule formulation and tubule branching were not affected in HUVECs which were transfected with anti-miR-296 AMO in nontargeted LPH-NP or mismatch AMO in cRGD-LPH-NP. Under these circumstances HUVECs differentiated into well-defined tubelike structures as shown in Figure 4A. In contrast, targeted delivery of anti-miR-296 AMO to HUVECs by cRGD-LPH-NP disturbed the formation of capillary-like structures. After 12 h incubation,

(41) Stern, K. A.; Smit, G. D. V.; Place, T. L.; Winistorfer, S.; Piper, R. C.; Lill, N. L. Epidermal growth factor receptor fate is controlled by Hrs tyrosine phosphorylation sites that regulate Hrs degradation. *Mol. Cell. Biol.* **2007**, *27*, 888–898.

(42) Bache, K. G.; Raiborg, C.; Mehlum, A.; Stenmark, H. STAM and Hrs are subunits of a multivalent ubiquitin-binding complex on early endosomes. *J. Biol. Chem.* **2003**, *278*, 12513–12521.

(43) Grant, D. S.; Kinsella, J. L.; Fridman, R.; Auerbach, R.; Piasecki, B. A.; Yamada, Y.; Zain, M.; Kleinman, H. K. Interaction of endothelial-Cells with a laminin-a chain peptide (sikvav) *in vitro* and induction of angiogenic behavior *in vivo*. *J. Cell. Physiol.* **1992**, *153*, 614–625.

(44) Ponce, M. L. *In vitro* Matrigel angiogenesis assays. In *Angiogenesis protocols*; Murray, J. C., Ed.; Humana Press: Totowa, NJ, 2001; pp 205−209.
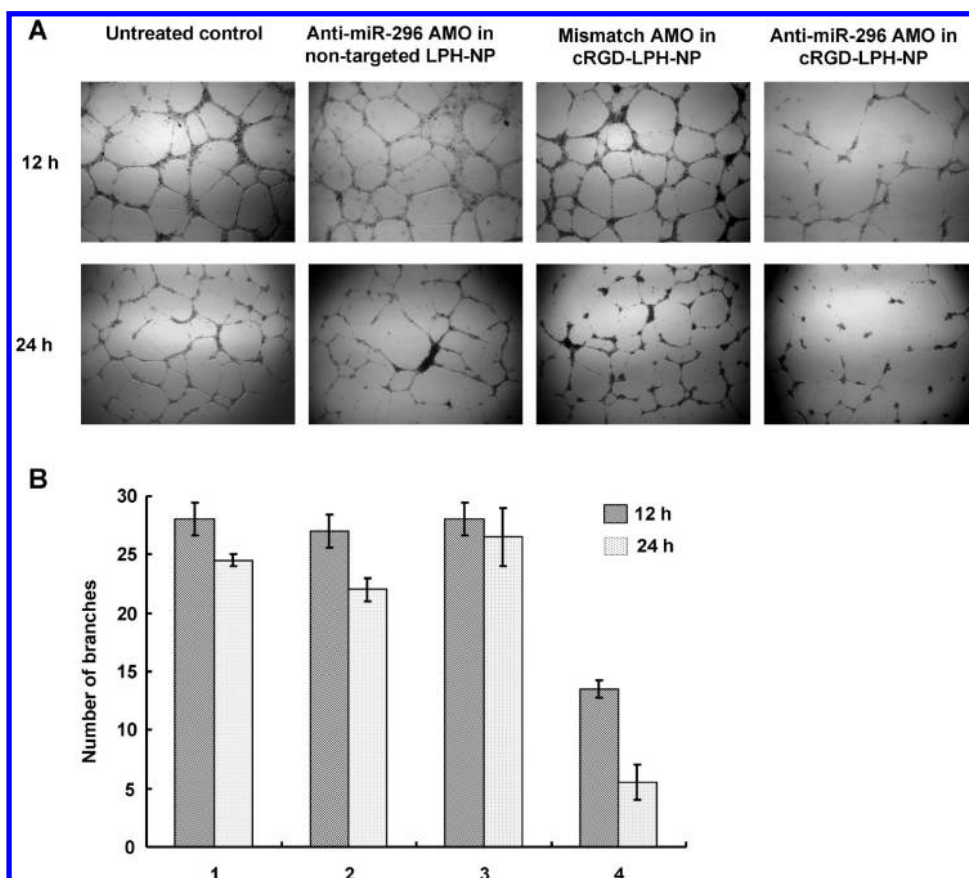
Figure 4. Inhibition on HUVEC tubule formation on Matrigel mediated by miR-296 following the delivery of anti-miR-296 AMO: (A) tube formation analysis of HUVECs after transfected with different formulations for 5 h and seeded onto Matrigel for 12 and 24 h incubation; (B) tubule formation was evaluated by the number of tubule branching after 12 and 24 h incubation on Matrigel. Each experiment was performed in triplicate (1, untreated control; 2, anti-miR-296 AMO in nontargeted LPH-NP; 3, mismatch AMO in cRGD-LPH-NP; 4, anti-miR-296 AMO in cRGD-LPH-NP).

HUVECs did not completely differentiate and instead only formed incomplete and short tubes. Meanwhile, there were almost no evident tubelike structures formed by HUVECs transfected with anti-miR-296 AMO in cRGD-LPH-NP after 24 h incubation. The antiangiogenesis potential of anti-miR-296 AMO in cRGD-LPH-NP was also demonstrated clearly by the number of tubule branches in Figure 4B.

In order to determine whether endothelial cell migration was also affected by targeted delivery of miR-296 AMO, scratch assay was performed. HUVECs were first transfected with different formulations containing anti-miR-296 AMO or mismatch AMO. After 5 h, a spatula was used to scratch the monolayer, and the cells were then washed and cultured in Medium 200 containing LSGS for 6 or 16 h. The migration distance was observed by a light microscopy (Figure 5). HUVECs transfected with anti-miR-296 AMO in cRGD-LPH-NP resulted in notably diminished potential in the migration during 6 h incubation. There was still an obvious wound after 16 h incubation; meanwhile in other groups the wounds had already been healed. Together, these data supported that only cRGD-LPH-NP could deliver anti-miR-296 AMO effectively to HUVECs and miR-296 silencing could reduce angiogenic phenotypes, suggesting that anti-

miR-296 AMO in cRGD-LPH-NP would be a good candidate for *in vivo* antiangiogenesis study.

3.5. *In Vivo* Antiangiogenesis Effects of Anti-miR-296 AMO Delivered by cRGD-LPH-NP. The Matrigel plug assay can be used to examine the function of angiogenesis inhibitors.[35−37] In this assay, Matrigel is premixed with basic fibroblast growth factor (bFGF) as an angiogenic compound, and the test substances are then added. Thus, the tested antiangiogenic substances inhibit the formation of vessels induced by bFGF in the Matrigel plug. The plugs removed from the mouse would be relatively colorless if the angiogenesis could be well prohibited.[45] We used the Matrigel plug assay to assess the antiangiogenic properties of different formulations containing either anti-miR-296 AMO or mismatch AMO *in vivo*. At 7 days following plug implantation, plugs containing bFGF alone displayed bright red color, indicating the formation of new blood vessels and blood circulation (Figure 6). Only slight decrease in microvessel formation within Matrigel was observed when plugs were mixed with anti-miR-296 AMO in nontargeted LPH-NP or mismatch AMO in cRGD-LPH-NP. The most significant inhibition of angiogenesis existed in plugs mixed with anti-miR-296 AMO in cRGD-LPH-NP, and the color of plugs
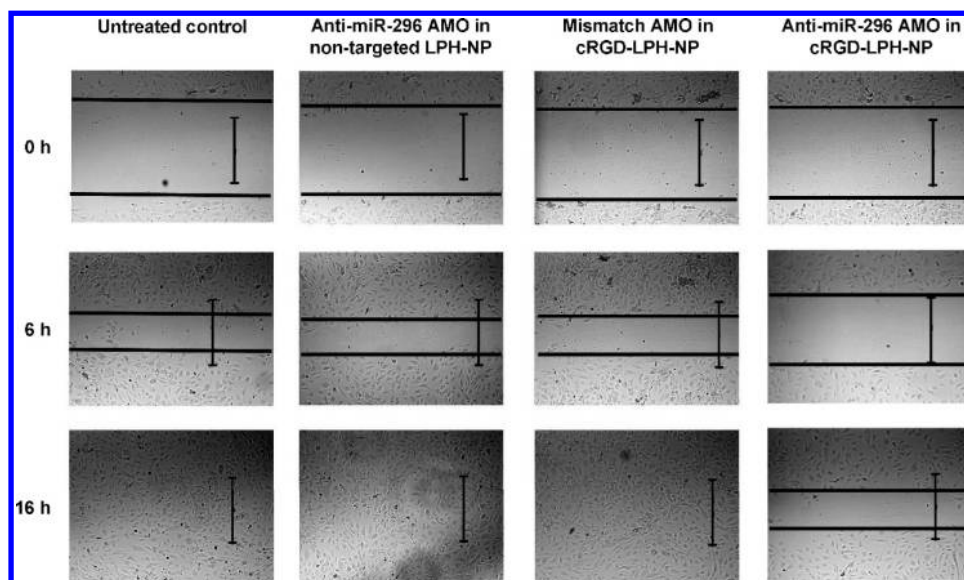
Figure 5. Inhibition on HUVECs' migration mediated by miR-296 following the delivery of anti-miR-296 AMO. The monolayer of HUVECs was wounded after 5 h transfection, and the healing was observed after 6 and 16 h incubation (scale = 200 μm).
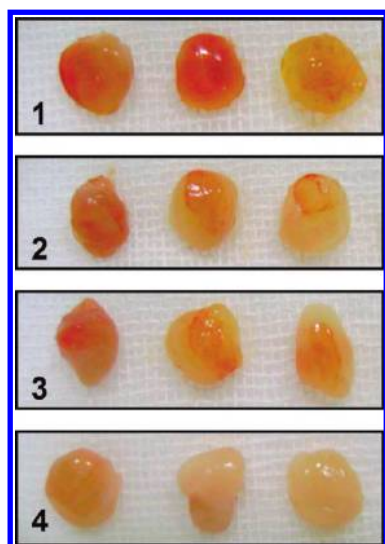

Figure 6. Angiogenesis in Matrigel plugs mediated by miR-296 following the delivery of anti-miR-296 AMO (1, untreated control; 2, anti-miR-296 AMO in nontargeted LPH-NP; 3, mismatch AMO in cRGD-LPH-NP; 4, anti-miR-296 AMO in cRGD-LPH-NP).

Figure 7. Immunohistochemical staining of HGS expressed by endothelial cells in Matrigel plugs mixed with different formulations (1, untreated control; 2, anti-miR-296 AMO in nontargeted LPH-NP; 3, mismatch AMO in cRGD-LPH-NP; 4, anti-miR-296 AMO in cRGD-LPH-NP).

was totally pale. These results implied that cRGD-LPH-NP was internalized by $\alpha_v\beta_3$ integrin-positive blood vessel endothelial cells through receptors, and then silencing of miR-296 inhibited cell proliferation and microvessel formation.

We further examined HGS expression within Matrigel plugs. Immunohistochemical staining revealed that HGS increased much more significantly in the plugs mixed with
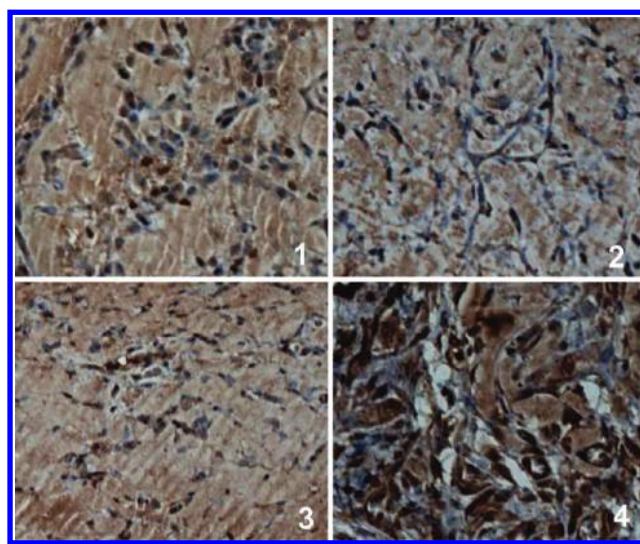
anti-miR-296 AMO delivered by cRGD-LPH-NP due to much more efficient miR-296 silencing as compared with other groups (Figure 7).

On the other hand, the Matrigel microenvironment contains a variety of extracellular matrix proteins and an angiogenic stimulus, basic FGF. This matrix may replicate at least in part in the environment which the tumor cells create *in vivo*.[46] The endothelial cells that migrate into Matrigel plugs (Matrigel-derived endothelial cells (MDEC)) were identified as an enriched population of endothelial cells which express PECAM-1 (CD31), a surface marker characteristic of endothelial cell lineage.[46] Thus, we used CD31 immunostaining

(45) Malinda, K. M. *In vivo* Matrigel migration and angiogenesis assays. In *Angiogenesis protocols*; Murray, J. C., Ed.; Humana Press: Totowa, NJ, 2001; pp 47−52.
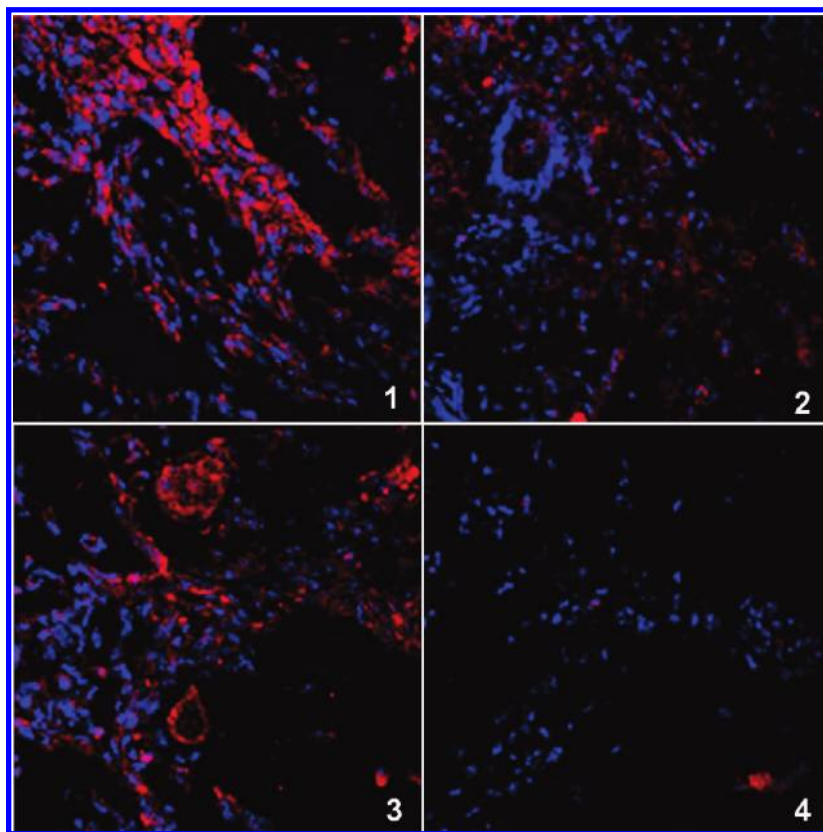
Figure 8. CD31-positive microvessel assessment of Matrigel plugs mixed with different formulations (red, rhodamine-labeled CD31-positive endothelial cells; blue, DAPI stained nuclei). 1: Untreated control. 2: Anti-miR-296 AMO in nontargeted LPH-NP. 3: Mismatch AMO in cRGD-LPH-NP. 4: Anti-miR-296 AMO in cRGD-LPH-NP.

to demonstrate MDEC invasion in Matrigel plugs mixed with different formulations containing either anti-miR-296 AMO or mismatch AMO. There were a lot of CD31-positive MDEC confirmed by red fluorescence within Matrigel plugs containing bFGF as the positive control (Figure 8). Much less red fluorescence labeled MDEC existed in plugs mixed with anti-miR-296 AMO in cRGD-LPH-NP when compared with those with anti-miR-296 AMO in nontargeted LPH-NP or mismatch AMO in cRGD-LPH-NP, which proved that anti-miR-296 AMO in cRGD-LPH-NP significantly suppressed the invasion of MDEC into Matrigel. Meanwhile, cells in the plugs, which were CD31 negative, might be pericytes or stromal cells that were recruited during neovascularization, which may play a role in endothelial cell proliferation, survival, permeability, migration and maturation.[47]

The antiangiogenic studies demonstrated that cRGD-LPH-NP more effectively interacted with $\alpha_v\beta_3$ integrin-positive endothelial cells, leading to efficient delivery of anti-miR-296 AMO. Indeed, anti-miR-296 AMO in cRGD-LPH-NP more significantly inhibited CD31-positive MDEC migration and microvessel formulation in Matrigel plug models. Therefore, cRGD-LPH-NP holds great potential for targeted delivery of anti-miR-296 AMO to endothelial cells for antiangiogenic therapy.

4. Conclusion

We have developed a PEGylated LPH nanoparticle system functionalized with cRGD for specific and efficient delivery of anti-miR-296 AMO into $\alpha_v\beta_3$ integrin-positive endothelial cells. The targeted nanoparticles exhibited effective antiangiogenesis activities of suppressing blood tube formulation and endothelial cell migration both *in vitro* and *in vivo*. These findings could encourage further investigation of targeted delivery of other miRNA or anti-miRNA AMO with the same or similar delivery system for effective antiangiogenesis therapy for various types of cancer.

(46) Chung, I.; Wong, N. K.; Flynn, G.; Yu, W. D.; Johnson, C. S.; Trump, D. L. Differential antiproliferative effects of calcitriol on tumor-derived and matrigel-derived endothelial cells. *Cancer Res.* **2006**, *66*, 8565–8573.

(47) Morikawa, S.; Baluk, P.; Kaidoh, T.; Haskell, A.; Jain, R. K.; McDonald, D. M. Abnormalities in pericytes on blood vessels and endothelial sprouts in tumors. *Am. J. Pathol.* **2002**, *160*, 985–1000.